Journal of Energy Storage 17 (2018) 327–335

Contents lists available at ScienceDirect

Journal of Energy Storage

journal homepage: www.elsevier.com/locate/est

Air supply temperature impact on the PEMFC impedance

Slimane Laribi[a,*], Khaled Mammar[b], Youcef Sahli[a,c], Khaled Koussa[a]

[a] Unité de Recherche en Energies Renouvelables en Milieu Saharien, URERMS, Centre de Développement des Energies Renouvelables, CDER, 01000, Adrar, Algérie
[b] Department of Electrical and Computer Engineering, University of Tahri Mohamed Béchar Bp 417, Algeria
[c] Département de Mécanique, Faculté de Technologie, Université de Batna 2, Algérie

ARTICLE INFO

Keywords:
Electrochemical impedance spectroscopy
Water management
Impedance model
PEMFC
Drying
Flooding

ABSTRACT

In this work, a neural network is used to optimize the impedance model of a proton exchange membrane fuel cell (PEMFC). In particular, the model is used to diagnose the effect of the air supply temperature on the water management and humidification of the fuel cell, for an interval of air supply temperature of 60–140 °C to predict the hydration state of the fuel cell (flooding and drying). The Multi-Layer-Perceptron through back propagation training algorithms of the neural network model satisfactorily predicts parameters (the mean square error value of ANN is $6.67\,e^{-16}$). The neural network method is applied to investigate the PEMFC impedance under drying and flooding conditions. The proposed model is validated by the experimental results of the literature at a frequency range of 0.1 Hz–1 kHz, RH = 10%, t = 180 s for drying case and RH = 100%, t = 500 and 1600 s for flooding case. The proposed approach enabled us to identify the five physical parameters of the impedance that exhibited high sensitivity in the PEMFC diagnostic (the membrane resistance, the polarization resistance, the double layer capacitance of the electrode/electrolyte interfaces, the resistance of species diffusion and the time constant of the charges diffusion).

1. Introduction

For some years, the declining fossil energy resources have directly led to the search for other energy sources having the same properties as the hydrocarbons in terms of storage and transport. In this context, hydrogen turns out to be a very strong candidate, even if he is only an energy carrier and not a primary resource. Hydrogen, which does not exist in nature, may indeed be synthesized by the use of renewable energies. Besides its function as an energy carrier, his storable character can be used to meet the requirements of energy consumers. Among its main uses, hydrogen is used as fuel in the fuel cells field, the latter has been accepted as a prospective alternative for energy nowadays, they are not a new technology, and their principle was discovered in the first half of the 19th century. Sir William Grove is considered the inventor of the fuel cell by his famous experiment performed in 1839. The today fuel cell represents a considerable challenge in the development of renewable energies. Indeed, these cells, therefore have a clear environmental benefit.

Several types of fuel cell exist which are classified depending on the nature of the electrolyte, the operating temperature and the conductor type. Among all his existing families, a particular attention is given to the cells which have a membrane of polymer, an exchange of the protons and a low operate temperature (PEMFC), which are used by NASA in the sixties in the Gemini space program [1]. The PEMFC is considered currently as the best adapted to the automotive sector. Among its strengths, the dynamics compared to other cell types, the low operating temperature of 40–100 °C and the easy integration into a vehicle without specific thermal insulation [2,3]. A PEM fuel cell consists of an anode, a cathode separated by a hydrated polymer as an electrolyte (membrane). It permits to transform the chemical energy of a gas or a fuel into electrical energy. The fuel used in most fuel cells is the hydrogen. Methanol can also be used directly in some fuel cell types [4].

In hydrogen fuel cells; the conversion of the chemical energy into electrical energy is carried out simultaneously with the water and heat production; it is performed by a chemical reaction of redox type. The hydrogen combines with oxygen to form the water according to the following general equation [2,3,5]:

$$H_2 + 1/2O_2 \rightarrow H_2O + \text{Heat} + \text{electrical energy} \quad (1)$$

At the anode, hydrogen is decomposed into electrons and protons. The membrane that is impermeable to gases, passes only protons. Electrons are driven from the anode to the cathode through an external

Abbreviations: ANN, artificial neural network; CPE, constant phase elements; DMFC, direct methanol fuel cell; EIS, electrochemical impedance spectroscopy; PEM, proton exchange membrane; PEMFC, proton exchange membrane fuel cell; RH, relative humidity (%)

* Corresponding author.
E-mail address: laribi.slimane@urerms.dz (S. Laribi).

https://doi.org/10.1016/j.est.2018.03.020
Received 27 October 2017; Received in revised form 29 March 2018; Accepted 29 March 2018
Available online 05 April 2018

Nomenclature

b_i	Input bias of ANN
C	Oxygen concentration in cathode active layer (mol m^{-3})
C_{dl}	Double layer capacitance (F)
D	Diffusion coefficient (m^2 s^{-1})
f	Signal frequency (Hz)
F	Faraday number (A s mol^{-1})
if_c	Fuel cell current (A)
Im	Imaginary axe (Ω)
j	Imaginary number
n	Electron numbers
q_{O2out}	Oxygen molar flow at the output (mol s^{-1})
q_{O2in}	Oxygen molar flow at the cell input (mol s^{-1})
q_{rest}	Molar flow of the non-oxygen (mol s^{-1})
q_{win}	Water molar flow introduced by the air (mol s^{-1})
q_{wprod}	Produced water molar flow (mol s^{-1})
P_{exit}	Pressure at the stack output (bar)
P_{in}	Total inlet air pressure (bar)
P_{sat}	Saturated vapor pressure (bar)
P_{win}	Water vapor pressure at the cell inlet (bar)
P_{wout}	Water vapor partial pressure (bar)
Q	CPE parameter or double layer capacitance at the electrode/electrolyte interface (S s$^{\alpha}$)
R	Perfect gas constant (J mol^{-1} K^{-1})
R_d	Diffusion related resistance (Ω)
Re	Real axe (Ω)
R_{int}	Internal resistors measured at high frequency (Ω)
R_m	Electrolyte ohmic resistance (Ω)
R_p	Polarization resistance (Ω)
R_{pol}	Biasing resistor measured at low frequency (Ω)
S	Active area (m^2)
T	Temperature (°C)
T_{air}	Air supply temperature (°C)
w_{ij}	Synaptic weights of neuron j
x_i	Input signal
Z_{cell}	Fuel cell impedance (Ω)
Z_{CPE}	CPE impedance (Ω)
Z_w	Warburg impedance (Ω)

Greek letters

λ	Air stoichiometry
ΔI	Current variation (A)
ΔU	Perturbation voltage (V)
α	CPE power value
τ_d	Diffusion time constant (s)
ω	Pulsation (rad s^{-1})
δ	Diffusion layer width (m)

circuit. At the cathode, the oxygen combines with the protons and electrons to produce the water. The overall reaction (Eq. (1)) can be decomposed in this case in two half-reactions, which take place respectively at the anode and at the cathode Fig. 1:

$$2H_2 \rightarrow 4H^+ + 4e^- \text{ Anode} \quad (2)$$

$$O_2 + 4e^- \rightarrow 2O^{2-} \text{ Cathode} \quad (3)$$

Water production is one of the results of the electrochemical reaction, allowing to say that water management is essential for the ideal operation of a PEM fuel cell. The membrane must always remain saturated with water to allow the movement of H^+, it is the most important aspect of the operation of this cell type. The water management plays a crucial role in the functioning diagnosis of PEMFC; it's one of the questions paramount because a lack of water can lead to the drying of the membrane, which directly leading to the fuel cell destruction, conversely, an excess of water will decrease the species transport at the PEMFC heart, and this causes the yield inevitable reduction. Therefore, it is important to control the humidity to ensure that the humidification and the water evacuation are sufficient for a proper hydration of the membrane without any risk of saturation or engorgement of the PEMFC [6,7].

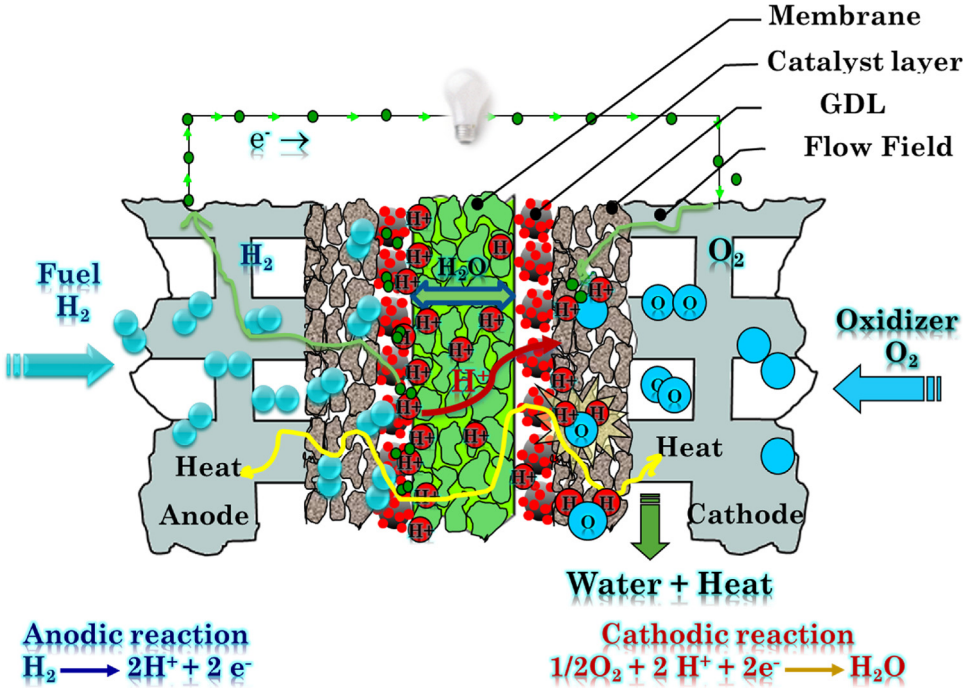

Fig. 1. Basic operation of PEMFC.

The impedance spectroscopy is the analysis tool for the limitation of material transport to the electrodes, precisely to the cathode of the PEMFC that is supplied by the air generally. The impedance spectroscopy is used to control the impact of the operating conditions: pressure, temperature, flow and membrane humidity [5,8,9]. The frequency behavior also shows the specific singularities of certain phenomena. The impedance measurement is used to follow the degradation of the fuel cell membranes (e.g., an increase in the impedance in the event of membrane failure) [10,11]. The system approach has been chosen for measuring the PEMFC global impedance according to the frequency to deduce an electrical model of the cell in charge [10,11].

We rely on the results obtained by Fouquet et al. [7] that are used to describe the evolution of the parameters of the model during the drying or flooding, that they provoked voluntarily in the cell. During each phase of degradation, they are realizing the impedance spectroscopy to characterize the impedance and follow the produced change. The variation of certain parameters enabled to differentiate between flooding and drying of the cell. Slepski et al. [13] have studied a complete electrochemical impedance system composed by two electrodes and one membrane which enables to determine separately the system impedance instantaneous value. This technique is verified by the simulation of the equivalent electrical circuit. Slepski et al. [14] have studied the direct methanol fuel cell (DMFC) behavior electrochemical using an electrochemical impedance method that optimizes the fuel cell performance and detects the fuel cell defects.

The objective of the present work is to present and implement a new method to analyze and diagnose the air supply temperature impact on the water management in the PEMFC. This method is based on a Randles physical model improved by a constant phase element (CPE) to develop a fuel cell theoretical model which is based on the impedance in order to evaluate the influence of air supply temperature on the allocation of water and the reagents in the PEMFC heart. The electrochemical impedance model parameters are obtained from the EIS experience in both studied cases: drying and flooding of the cell membrane. For this work, the ANN are used for creating the optimal impedance model of the PEM fuel cell to find better physical parameter estimations of the electrochemical impedance. The estimated circuit parameters gives information about the membrane hydration.

2. Impedance fuel cell model formulation

The simplest representation of PEMFC fuel cell in the form of an electric model consists in putting a direct voltage source in series with an electrical impedance. In this paper, we will proceed to determinate and diagnose of this Z_{cell} impedance.

2.1. Impedance spectroscopy principle

Electrochemical impedance spectroscopy is a non-stationary technique based on the reactive phenomena differentiation by their relaxation time. The electrochemical system is submitted to a sinusoidal voltage perturbation of low amplitude and variable frequency [15]. At each frequency, the various processes evolve according to different rates, enabling to make a distinguish them. The weak sinusoidal perturbation amplitude is superimposed generally with the corrosion potential or the open circuit potential Fig. 2:

$$\Delta U = |\Delta U| \sin\ \omega t \quad \text{With} \quad \omega = 2\pi f \tag{4}$$

Where f is the applied signal frequency (Hz). ΔU is the perturbation, which induces a sinusoidal current. ΔI is the current variation which has a phase shift with respect to the potential:

$$\Delta I = |\Delta I| \sin(\omega t - \varphi) \tag{5}$$

These values can be represented in the complex plane:

$$\Delta U = \Delta U_{re} + i\Delta U_{im} \tag{6}$$

$$\Delta I = \Delta I_{re} + i\Delta I_{im} \tag{7}$$

The complex impedance is defined by:

$$Z = \frac{\Delta U}{\Delta I} = Z_{re} + iZ_{im} \tag{8}$$

In addition, the impedance can be represented by the modulus $|Z|$and the phase angle shift φ:

$$|Z| = \sqrt{Z_{re}^2 + Z_{im}^2} \tag{9}$$

$$\varphi = \arctan\left(\frac{Z_{im}}{Z_{re}}\right) \tag{10}$$

2.2. PEM fuel cell impedance model

Since 1947, the model developed by Randles for the representation of phenomena produced in the interfaces between the electrodes and the electrolyte is supposed to be valid; it is composed of an electrolyte resistance in series with a circuit composed of a double-layer capacitor in parallel with a serial charge transfer resistance with a Warburg impedance Fig. 3a. In 2006, Fouquet et al. [7] have enhanced the Randles model to use it in the fuel cell control domain, this improvement consists essentially of a replacement of the double layer capacity by a constant phase element (CPE) Fig. 3b. This improvement renders the circuit capable to capture all action with very a little error compared with the classic Randles model.

According to the equation of Butler-Volmer and the second law of Fick, the diffusion impedance equation for a finite length diffusion layer is presented by the following equation [7,12,16–20]:

$$Z_w(j\omega) = \frac{RT\delta}{n^2F^2SCD}\frac{\tanh\sqrt{j\omega(\delta^2/D)}}{\sqrt{j\omega(\delta^2/D)}} \tag{11}$$

The Eq. (11) can be written as [7,12,18–20]:

$$Z_w(j\omega) = R_d\frac{\tanh\sqrt{\tau_d j\omega}}{\sqrt{\tau_d j\omega}} \tag{12}$$

Where τ_d is the diffusion time constant, which is given by the ratio between the diffusion layer width and the diffusion coefficient ($\tau_d = \delta^2/D$) and R_d is the diffusion resistance, it is given by the following equation [7,12,18–21]:

$$R_d = \frac{RT\delta}{n^2F^2SCD} \tag{13}$$

Fuel cell impedance consists of two impedances at each electrode

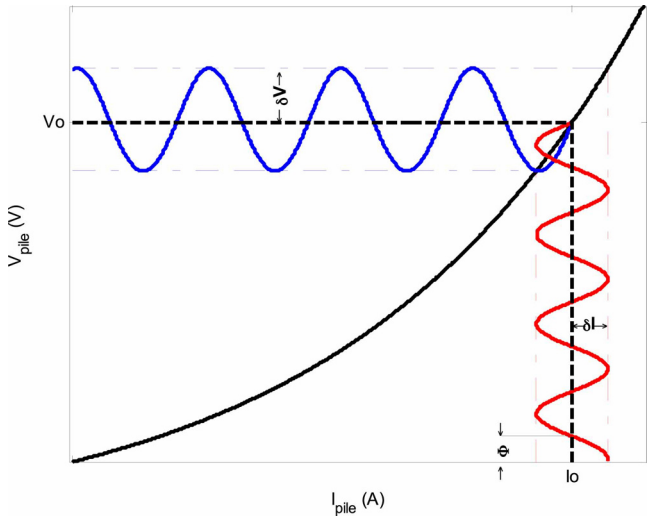

Fig. 2. Linearization principle around of the operating point.

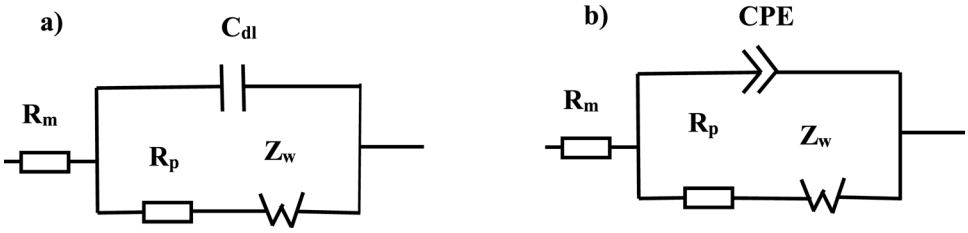

Fig. 3. Equivalent circuit. a) Randles model, b) Fouquet improvement.

(cathode and anode). These impedances are situated after the membrane internal resistance. According to Fouquet et al. [7], Mammar et al. [12], the reaction rate limiting is linked to the oxygen reduction at the cathode, also, anode impedance contribution is neglected by – report to the total cell impedance. The PEMFC equivalent circuit model is represented in Fig. 3b. The cell total impedance is given by the following equation:

$$Z_{cell}(j\omega) = R_m + \frac{1}{Z_{CPE} + (1/(R_{..P} + Z_w))} \tag{14}$$

The constant phase element impedance is defined by [7,12,18–20]:

$$Z_{CPE}(j\omega) = \frac{1}{Q(j\omega)^{\alpha}} \tag{15}$$

R_p is the polarization resistance, it characterizes the charge transfer phenomena to the electrodes. CPE power value varies between 0.5 and 1. Therefore, the equivalent circuit impedance is given by [18–21]:

$$Z_{cell}(j\omega) = R_m + \frac{1}{Q(j\omega)^{\alpha} + (1/(R_P + Z_w))} \tag{16}$$

For the model parameter identification, a nonlinear method that is based on the least square method, to identify all the parameters of the cell Randles. The used algorithm principle is based on the nonlinear function square minimization to find the unknown variable best values starting from their initial values that are given by Table 1 [7,12,18] for the cell flooding and drying (RH = 100%, RH = 10%).

2.3. Air humidity influence on PEMFC behavior

The fuel cell successful operation is linked to the water management (relative humidity), which must be optimal in any time, that is to say, the membrane must be has a specific humidity as a function of the temperature, pressure of air flow… etc., for avoiding all flooding or drying of the membrane and allow to ensure a better operation of the PEMFC. The air supply temperature is the most important parameter that has the greatest influence on the relative humidity of the PEMFC.

The air hydration at the PEMFC inlet can be turned into liquid water internally in the fuel cell. On the other hand, the exhaust air at the fuel cell outlet can evacuate the water at the cell outside. On the other hand, if the exhaust air has a relative humidity of 100%, then the exhaust air is really saturated and does not contain all the water quantity, which causes an undesirable accumulation of water in the cell. Conversely, if the exhaust air humidity is less than 100%, the cell membrane may be dried. In both cases, the efficiency of the PEMFC will be reduced.

PEMFC relative humidity should be less than 100% to avoid the accumulation of liquid water in both electrodes, but it should be more than 80%, to prevent the fuel cell membrane excessive drying. The question that arises, what are the conditions necessary to obtain this humidity?

Generally, the relative humidity represents the amount of water vapor in the air, so that; 0% indicates that the air is totally dry, and 100% indicates that the air is saturated with water. The relative humidity is defined by the ratio between the water partial pressure and the saturated vapor pressure Eq. (17) [6,21]:

$$RH = \frac{P_{wout}}{P_{sat}(T_{air})} \tag{17}$$

Where P_{wout} is the water vapor partial pressure and P_{sat} is the saturated vapor pressure.

The saturated vapor pressure is linked to the temperature change, it increases nonlinear way, according to the temperature value elevation [6,22]:

$$P_{sat} = 10^5 \exp\left(13.7 - \left(\frac{5120}{T_{air} + 273.15}\right)\right) \tag{18}$$

In a gaseous mixture, each gas partial pressure is given by the rapport between the molecule number of this gas and the molecule total number of the mixture [6,21]:

$$\frac{P_{wout}}{p_{exit}} = \frac{\text{number of water molecules}}{\text{total number of molecules}} \tag{19}$$

$$\frac{P_{wout}}{p_{exit}} = \frac{q_{win} + q_{Wprod}}{q_{win} + q_{Wprod} + q_{O2out} + q_{rest}} \tag{20}$$

Where q_{win} is the water molar flow introduced by the air (mol s^{-1}), q_{wprod} is the produced water molar flow (mol s^{-1}), q_{O2out} is the oxygen molar flow at the output, q_{rest} the molar flow of the non-oxygen component (N2) of air and P_{exit} is the pressure at the stack output, and it is equal to the atmospheric pressure.

$$q_{Wprod} = \frac{if_c}{2F} \tag{21}$$

$$q_{O2out} = (\lambda - 1)\frac{if_c}{4F} \tag{22}$$

$$q_{win} = \Psi.(q_{O2in} + q_{rest}) \tag{23}$$

Where Ψ is a simplification coefficient, it is defined by the following pressure rapport:

$$\Psi = \frac{P_{win}}{P_{in} - P_{win}} \tag{24}$$

Where P_{win} is the water vapor pressure at the cell inlet and P_{in} represent the total inlet air pressure.

q_{O2in} is the oxygen molar flow at the cell input, it is defined by the product of the half of the consumed oxygen molar flow q_{wprod} and the air stoichiometry λ, if_c is the fuel cell current (A) and F is the Faraday number.

$$q_{O2in} = \lambda\frac{if_c}{4F} \tag{25}$$

Table 1
Model parameters during the cell drying and flooding [7,12,18].

Time(sec)	RH (%)	R_m (ohm)	Q (S s^{α})	R_p (ohm)	R_d (ohm)	τ_d (sec)	U(V)
500	10	0.00512	0.952	0.0099	0.0051	0.1155	4.06
3700	10	0.0088	0.62	0.013	0.0101	0.1835	3.35
500	100	0.00398	1.109	0.008	0.0034	0.0872	4.18
3700	100	0.00416	0.936	0.0163	0.0312	0.0947	3.3

$$q_{rest} = \frac{100 - O_{2\%}}{O_{2\%}} \lambda \frac{if_c}{4F} \tag{26}$$

For the air as oxidize, the molar flow of the non-oxygen component is given by:

$$q_{rest} = \frac{100 - 21}{21} \times \lambda \frac{if_c}{4F} = 3.76\lambda \frac{if_c}{4F} \tag{27}$$

Eq. (20) can be written as (28) [6,21]:

$$\frac{P_{wout}}{P_{exit}} = \frac{\Psi\left(\lambda \frac{if_c}{4F} + \frac{100 - O_{2\%}}{O_{2\%}} \lambda \frac{if_c}{4F}\right) + \frac{if_c}{2F}}{\Psi\left(\lambda \frac{if_c}{4F} + \frac{100 - O_{2\%}}{O_{2\%}} \lambda \frac{if_c}{4F}\right) + \frac{if_c}{2F} + (\lambda - 1)\frac{if_c}{4F} + \frac{100 - O_{2\%}}{O_{2\%}} \lambda \frac{if_c}{4F}} \tag{28}$$

For the air as oxidize, the water vapor partial pressure is given by the following equation:

$$P_{wout} = \frac{(0.420 + \lambda\Psi) P_{exit}}{\lambda(1 + \psi) + 0.210} \tag{29}$$

Finally, the relative humidity defined by Eq. (17) can be written as:

$$RH = \frac{P_{wout}}{P_{sat}(T_{air})} = \frac{\frac{(0.420 + \lambda\Psi) P_{exit}}{\lambda(1 + \psi) + 0.210}}{10^5 \exp\left(13.7 - \left(\frac{5120}{T_{air} + 273.15}\right)\right)} \tag{30}$$

3. Dynamic characterization of the fuel cell by ANN

The ANN principle is founded on the approximation of functions. In the present study, an ANN of type feed-forward with a supervised training is used to create the neural network. This ANN is based on the following four steps:

- Construction of ANN block.
- Learning base (data acquisition).
- Defect classifications.
- Test of network.

The used ANN in our work consists of three layers, the first is the input layer, the second is the hidden layer and the third is the output layer. In the network, each neuron is logically linked to the next layer neurons Fig. 4a.

The sigmoid function is used in the hidden layer as a transfer function; it is given by the following equation [18,23]:

$$f(u) = \frac{1}{1 + e^{-(d.u)}} \tag{31}$$

Where d is the curve steepness. The hidden layer input is given by the following equation [23]:

$$u = \sum_{j=1}^{n} (w_{ij} x_i + b_i) \tag{32}$$

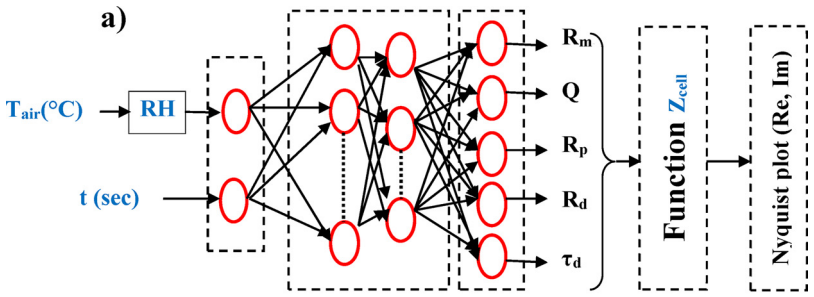

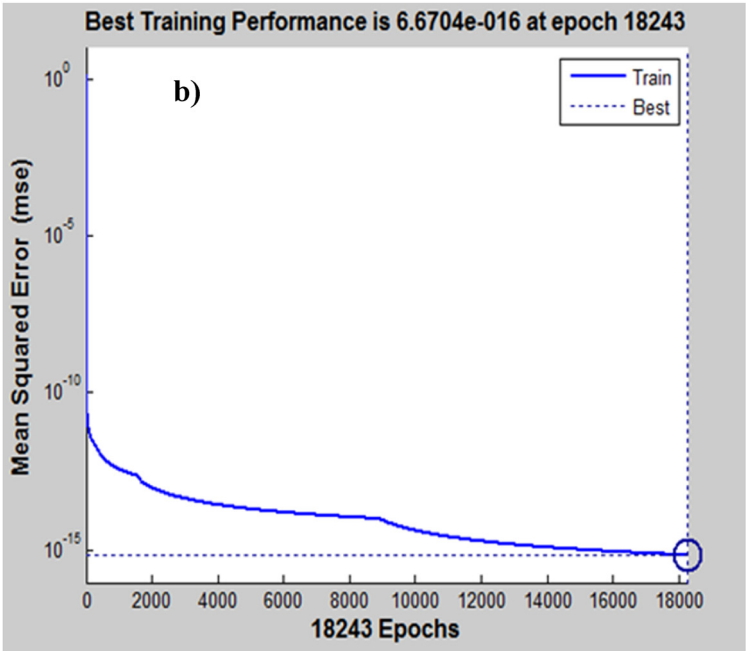

Fig. 4. PEMFC impedance ANN. a) ANN architecture, b) ANN squared errors.

Where x_i represents the input signal, w_{ij} are the synaptic weights of neuron j, their role is the simulation of the synaptic weights with the respectively associated weights to each neuron input. These weights weigh inputs and can be modified by learning, b_i is the bias input often takes the value -1 or $+1$.

For an output layer function linear, the equation that represents the network model is given by [18,23]:

$$y_k u = \sum_{j=1}^{N} (w^0{}_{ij} u_i + b_i) = \sum_{j=1}^{N} w^0{}_{ij} f\left(\sum_{j=1}^{N} (w_{ij} x_i + b_i)\right) \quad (33)$$

Where y_k is the output signal from k^{th} output neuron, $w^0{}_{ki}$ is the weight of i^{th} output u_i to the k^{th} neuron in the output layer. In the present work, the values of neural network bias and the weight are updated according to the algorithm of dynamic gradient descent [21,24].

Fig. 4a presents the ANN model architecture. The ANN input layer part is constituted by two neurons, the first input neuron is bound to the relative humidity that is given in function of the air supply temperature (Eq. (31)) and the second input neuron is bound to the operation time. The hidden layer part consists of two under layers of 20 neurons for the first under layer and 10 neurons for the second under layer. Finally, the output layer is constituted to 5 neurons. For proceed to the impedance physical parameter simulation, we proceed to complete the MATLAB code development that's based on the previously presented model by using the Neural Networks Toolbox of MATLAB. The function "tansig" (hyperbolic tangent sigmoid transfer) is used in the MATLAB code for estimations of the hidden layer parameters, the function "purelin" (linear transfer) is used in the estimations of the output layer parameters. The network training performance in terms of Mean Squared Error (MSE value) and iteration value (EPOCHS) are shown in Fig. 4b.

Once ANN learning of impedance is done; the neural network block of the impedance is generated by the function "gensim", this block represents the estimator of the physical parameters of the fuel cell impedance. The estimated values by the impedance block are the physical parameters of the developed Randles model. (R_m, Q, R_p, R_d, τ_d). The input values of the impedance ANN are the relative humidity RH (%) calculated by (Eq. (31)) and the operating time t (sec). For any relative humidity or air supply temperature, the impedance model is able to easily give the evolution of the PEMFC impedance physical parameters. Finally, these parameters are transmitted to the Eq. (16) to generate the Nyquist diagram, in order to diagnose the fuel cell hydration state.

4. Test and validation of the model

The used parameter values in the ANN learning step are shown in Table 1, for both studied cases; drying and flooding of the cell heart, this parameter values are taken from the reference [7]. In this learning, the least square method is used to identify the parameters of the Randles model enhanced by Fouquet et al. [7].

After the realization of the impedance ANN learning, we have proceeded to test of the obtained results, by their comparison with the experimental results of Fouquet et al. [7] for both studied cases; flooding and drying of the fuel cell heart.

In the cell heart flooding case, two validation tests with the experimental results of Fouquet et al. [7] are presented; the input necessary parameters for the first test are the time 500 s and the relative humidity RH = 100% in the frequency range of 0.1 Hz to 1 kHz. In the second test, the input necessary parameters are the time 1600 s and the relative humidity RH = 100% in the frequency range of 0.1 Hz to 1 kHz.

In the cell heart drying case, the input parameters are taken from the Fig. 10 presented by Fouquet et al. [7], where the time is about 180 s and RH is 10%, in a frequency range of 0.1 Hz to 1 kHz.

The experimental results and the model results are presented in Fig. 5, the comparisons between experimental and numerical results of each test indicate that the used procedure is reliable.

5. Results and discussion

For proceed to the PEMFC ANN impedance model simulation in a time variation of (10 min to 1 h) at the dry condition, we introduce in every simulation; the time and humidity relative that is calculated by (Eq. (31)). After the simulation of the ANN impedance model, we obtain an estimate of the Randles model parameters with CPE (R_m, Q, R_p, R_d, τ_d), these parameters are directly used to Z_{cell} function calculation that is used by "Nyquist plot MATLAB" for the curve plots (Re, $-$Im).

The fuel cell impedance Nyquist diagram spectra characterize the drying effect of the membrane, Fig. 6a. These specters gradually shift to the right side of the real axis in operation time function at the high frequency part, also, a loop size enlargement in the low frequency part that is logically explained by the increase in the fuel cell membrane resistance.

In Fig. 6b the fuel cell impedance Nyquist diagram spectra characterize the membrane flooding effect. For low frequencies, a large expansion of the loop size is presented by the attachment to the diffusion process. In high frequency part, we note a small change in the arcs that is due to the membrane resistance limitation.

The air supply temperature has a direct effect on drying and

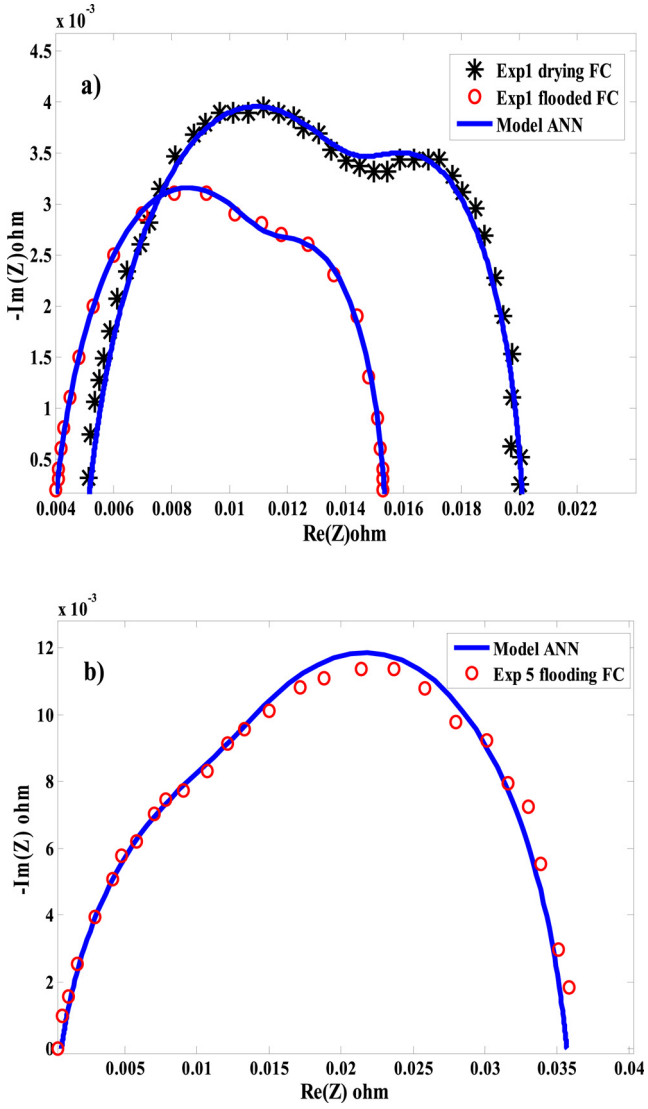

Fig. 5. Model validation. a) Drying case, b) Flooding case.

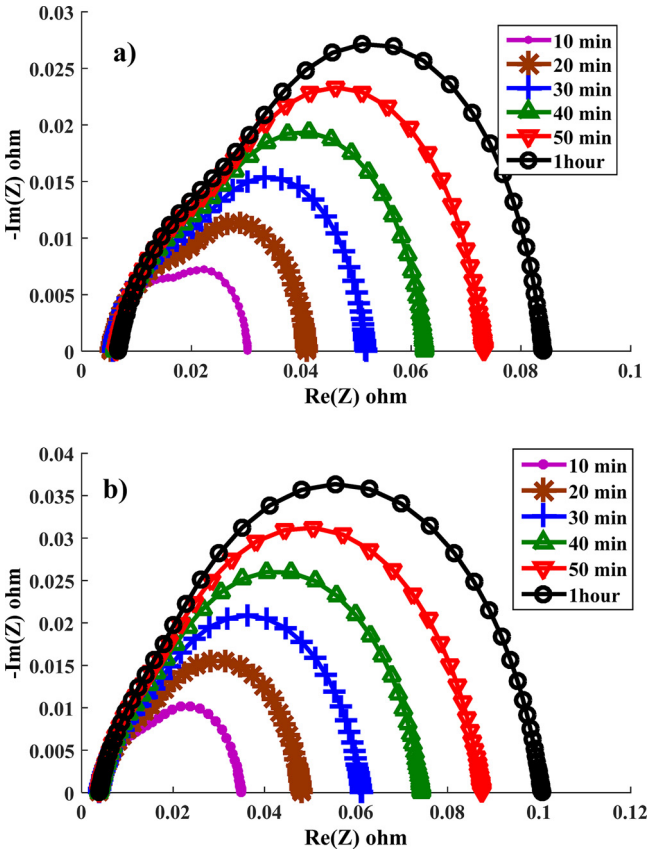

Fig. 6. PEMFC Nyquist diagram according to the different operating time. a) Drying case, b) Flooding case.

flooding of fuel cell membrane that is clearly shown in the impedance spectra Fig. 7a,b . The increase of temperature causes a gradual slip of the spectra to the real axis right side as a time function, which also causes a water content reduction and a resistance increase in the membrane. The measured resistance at the low frequency of the cell is shown in Fig. 7a,b; this measured resistance gradually decreases with time when the oxidizer supply temperature increases.

For monitoring and diagnosis of the fuel cell health state in the case of flooding or drying of the cell heart, we followed the evolution of five parameters (R_m, Q, R_p, R_d, τ_d).

Fig. 8a shows that the membrane ohmic resistance value increases with the operating time when the air supply temperature increases from 60 °C to 140 °C. The main factor of the membrane resistance increase is due to the fuel cell membrane ionic conductivity which is related directly to the water content. When the cell air supply temperature increases, the membrane water content decreases, also the membrane ionic conductivity will decrease and R_{int} increases and R_{pol} decreases. These changes are directly related to the relative humidity variation that is provoked by the air supply temperature variation. In addition, the relative humidity has an impact on the mobility of the proton at high frequency.

Fig. 8b show the variation of the double layer capacitance of the electrode/electrolyte interfaces. The gradual decrease of the double layer capacitance according to the time is clearly visualized in Fig. 8b. In addition, this capacitance decreases when the air supply temperature increases.

Fig. 8c presents the polarization resistance behavior. The polarization resistance value increases according to time if the air supply temperature increases. In other words, the air supply temperature increasing provokes the decreasing of the membrane water content. Consequently, the membrane ionic conductivity decreases and the electrochemical kinetic increase, which conduct to a decrease in the charge transfer resistance.

Fig. 8d and e show that the diffusion ohmic resistance value and the diffusion time constant are changing inversely. In other words, the diffusion ohmic resistance value decreases according to the operating time if the air supply temperature increases from 60 °C to 140 °C. In addition, the diffusion time constant value increases in the same condition, in other words, when the diffusion ohmic resistance of species in GDL decreases, the diffusion time constant of species increases.

Fig. 8f shows the relative humidity varies depending on the air supply temperature. The membrane ionic conductivity of the PEMFC is related to its content of water, the oxidizer relative humidity in cathode increases when the air supply temperature decreases. In other words, if the membrane content of water increases, this led to an increase of the membrane ionic conductivity when the air supply temperature is low.

6. Conclusion

In this paper, the neural network technique is used to create the optimal model of PEM fuel cell to diagnose and analyze of the impact of the PEMFC air supply temperature on the humidification and the water management in its heart. This technique is based on the Randles equivalent electrical circuit with ameliorated by a CPE. A particular attention is given to the PEMFC water management diagnosis in both cases: drying and flooding of the fuel cell heart.

This model has shown its precision in the fuel cell electrical response over the large operating ranges.

This used approach has enabled us to identify the hydration status of PEMFC using one of five physical impedance parameters that showed high sensitivity in PEMFC diagnosis.

The monitoring status of hydration of the PEM fuel cells is

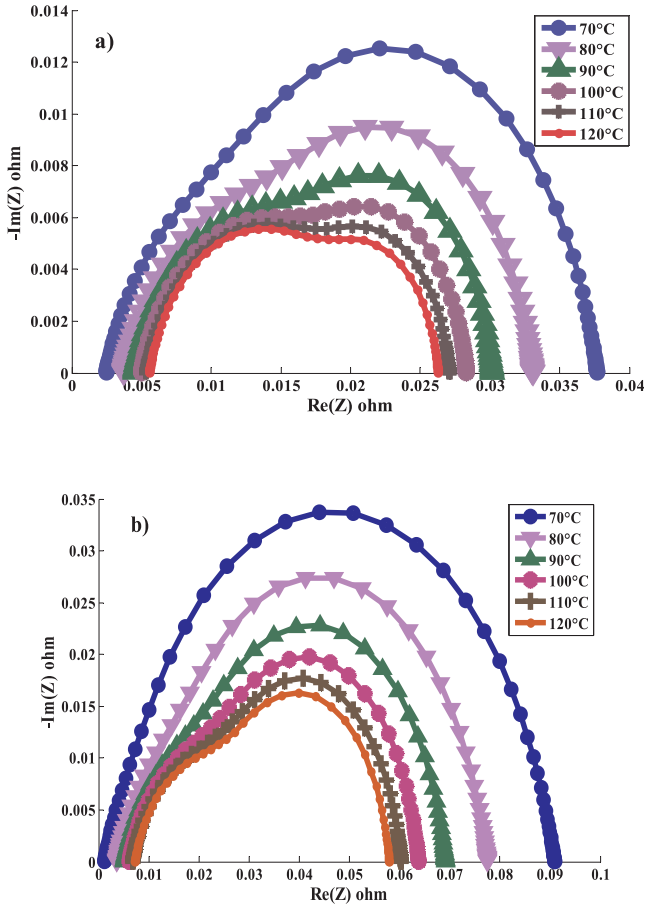

Fig. 7. PEMFC Nyquist diagram according to the different operating temperature. a) Drying case, b) Flooded case.

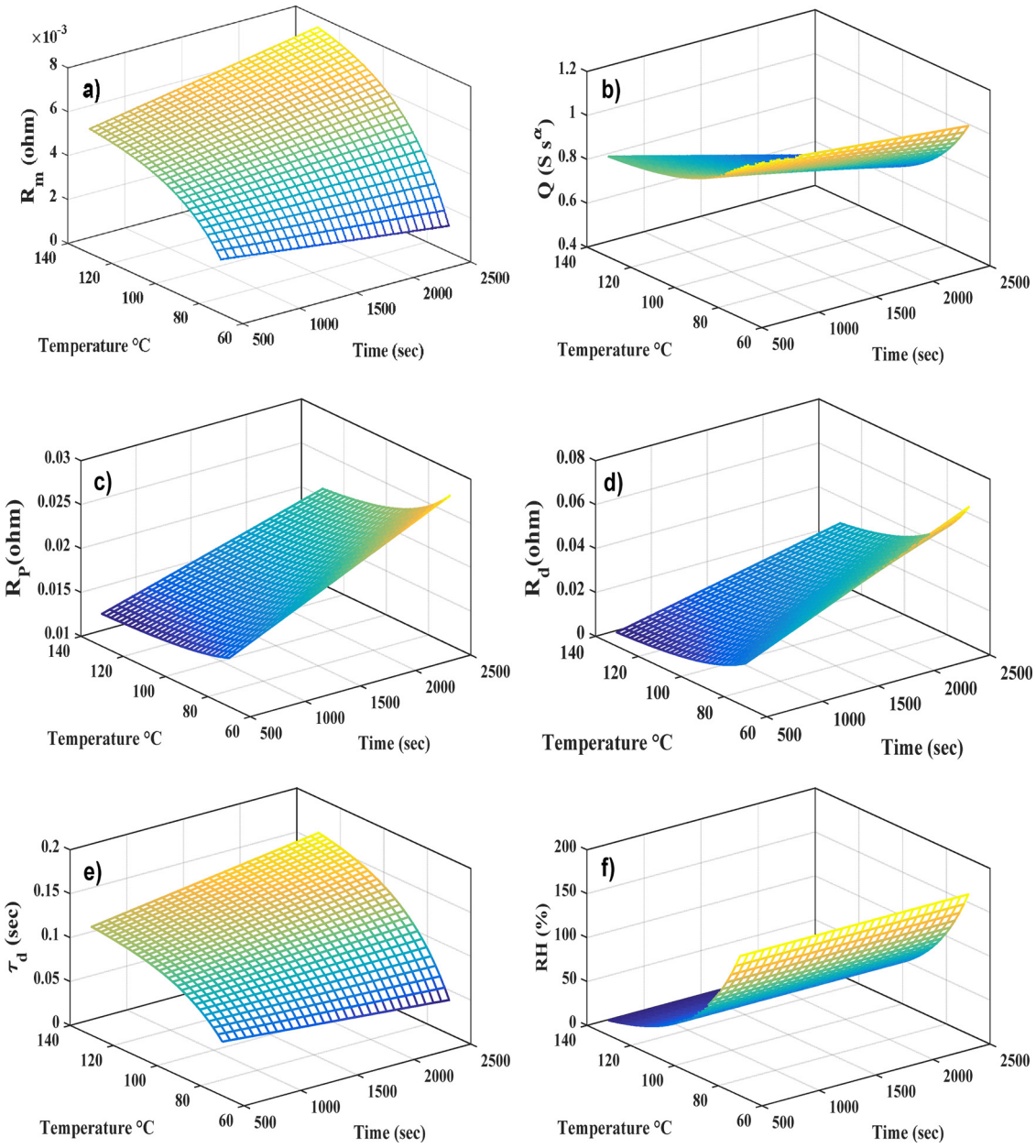

Fig. 8. Evolution of the model parameters according to the different time and operating temperature. a) R_m, b) Q, c) R_d, d) R_p, e) τ_d, f) $RH(\%)$.

demonstrated robust and very reliable under the measure of these five parameters of the impedance, the membrane resistance, the polarization resistance, the double layer capacitance of the electrode/electrolyte interfaces, the resistance of species diffusion and the time constant of the charges diffusion.

The effects analysis of the increase and decrease recorded in the air supply temperature values on the water management shows that:

- When the air supply temperature at the cathode increases the water content decreases at the cathode progressively, which also causes increases in the ohmic resistance of the membrane, the polarization resistance and the diffusion time constant. In addition, remarkable reductions of the diffusion resistance and the double layer capacitance of the electrode/electrolyte interfaces are obtained.
- When the oxidizer temperature decreases at the cathode, the water content increases in parallel, which leads to a logic decreases of the ohmic resistance of the membrane, the polarization resistance and the diffusion time constant and the evident increase of the diffusion resistance and the double layer capacitance of the electrode/electrolyte interfaces.

When the air supply temperature increases, the internal resistance is gradually reduced over time at high frequencies, in contrary, the polarization resistance at low-frequency increases gradually with time. In the case of decrease of the air supply temperature, the opposite is obtained.

References

[1] M. Rezaei Niya, M. Hoorfar, Study of proton exchange membrane fuel cells using electrochemical impedance spectroscopy technique, J. Power Sources 240 (2013) 281–293.
[2] J.M. Corrêa, F.A. Farret, L.N. Canha, M.G. Simões, An electrochemical-based fuel-cell model suitable for electrical engineering automation approach, IEEE Trans. Ind. Electron. 51 (5) (2004) 1103–1112.
[3] M.T. Outeiro, R. Chibante, A.S. Carvalho, A.T. De Almeida, A parameter optimized model of a proton exchange membrane fuel cell including temperature effects, J. Power Sources 185 (2) (2008) 952–960.

[4] W. Friede, S. Raël, B. Davat, Mathematical model and characterization of the transient behavior of a PEM fuel cel, IEEE Trans. Power Electron. 19 (5) (2004) 1234–1241.
[5] G. Mousaa, F. Golnaraghia, J. DeVaalb, A. Youngb, Detecting proton exchange membrane fuel cell hydrogen leak using electrochemical impedance spectroscopy method, J. Power Sources 246 (2014) 110–116.
[6] L. Boulon, K. Agbossou, D. Hissel, A. Hernandez, A. Bouscayrol, P. Sicard, M.C. Pera, Energy management of a fuel cell system: influence of the air supply control on the water issues, IEEE International Symposium on, IEEE Conference Publications (2010) 161–166.
[7] N. Fouquet, C. Doulet, C. Nouillant, G. Dauphin-Tanguy, B. Ould-Bouamama, Model based PEM fuel cell state-of-health monitoring via ac impedance measurements, J. Power Sources 159 (2) (2006) 905–913.
[8] J. Kim, I. Lee, Y. Tak, B.H. Cho, Impedance-based diagnosis of polymer electrolyte membrane fuel cell failures associated with a low frequency ripple current, Renew. Energy 51 (2013) 302–309.
[9] C. Brunetto, A. Moschetto, G. Tina, PEM fuel cell testing by electrochemical impedance spectroscopy, Electr. Power Syst. Res. 79 (1) (2009) 17–26.
[10] P. Agarwal, M.E. Orazem, L.H. Garcia-Rubio, Measurement models for electrochemical impedance spectroscopy I. Demonstration of applicability, J. Electrochem. Soc. 139 (7) (1992) 1917–1927.
[11] S.M. Rezaei niya, M. Hejabi, F. Gobal, Estimation of the kinetic parameters of processes at the negative plate of lead-acid batteries by impedance studies, J. Power Sources 195 (17) (2010) 5789–5793.
[12] K. Mammar, A. Chaker, Flooding and drying diagnosis of proton exchange membrane fuel cells using electrochemical impedance spectroscopy analysis, J. Electr. Eng. 13 (2013) 147–154.
[13] P. Slepski, K. Darowicki, E. Janicka, G. Lentka, A complete impedance analysis of electrochemical cells used as energy sources, J. Solid State Electrochem. 16 (2012) 3539–3549.
[14] P. Slepski, E. Janicka, K. Darowicki, B. Pierozynski, Impedance monitoring of fuel cell stacks, J. Solid State Electrochem. 19 (2015) 929–933.
[15] C. Gabrielli, Techniques de l'Ingénieur, traité Analyse et caractérisation, (2018) PE 2210-1:20.
[16] M.A. Danzer, E.P. Hofer, Analysis of the electrochemical behavior of polymer electrolyte fuel cells using simple impedance models, J. Power Sources 190 (1) (2009) 25–33.
[17] H. Girault, Electrochimie physique et analytique, Presses polytechniques et universitaires romandes, (2001).
[18] S. Laribi, K. Mammar, M. Hamouda, Y. Sahli, Impedance model for diagnosis of water management in fuel cells using artificial neural networks methodology, Int. J. Hydrogen Energy 41 (2016) 17011–17093.
[19] T. Miassa Amira, B. Olivier, G. Emmanuel, Identification of a PEMFC fractional order model, Int. J. Hydrogen Energy xxx (2016) 1–11.
[20] A. Saadi, M. Becherif, D. Hissel, H.S. Ramadan, Dynamic modeling and experimental analysis of PEMFCs: a comparative study, Int. J. Hydrogen Energy xxx (2016) 1–14.
[21] J.E. Larminie, A. Dicks, Fuel Cell Systems Explained Chichester, John Wiley and Sons, England, 2000.
[22] K. Agbossou, Y. Dube, N. Hassanaly, K.P. Adzakpa, J. Ramousse, Experimental validation of a state model for PEMFC auxiliary control, IEEE Trans. Ind. Appl. 45 (6) (2009) 2098–2103.
[23] H. Demuth, M. Beale, M. Hagan, Neural Network Toolbox ™ 6 User's Guide, Version 6.0.3. Copyright 1992-, The Math Works, Inc., 2009 ISBN: 0-9717321-0-8.
[24] F. Laurene, Fundamentals of Neural Networks, Architectures, Algorithms, and Applications, Prentice-Hall international editions, Prentice-Hall, 1994 ISBN: 0133341860 9780133341867.